



About the origins of NMR diffusion-weighting induced by frequency-swept pulses

Julien Valette^{a,b,c,*}, Franck Lethimonnier^c, Vincent Lebon^{a,b}

^a Commissariat à l'Energie Atomique (CEA), Institut d'Imagerie Biomédicale (I²BM), Molecular Imaging Research Center (MIRCent), 18 route du Panorama, BP n°6, Bât. 61, F-92265 Fontenay-aux-Roses, France

^b Centre National de la Recherche Scientifique (CNRS), Unité de Recherche Associée CEA-CNRS 2210, 18 route du Panorama, BP n°6, F-92265 Fontenay-aux-Roses, France

^c Commissariat à l'Energie Atomique (CEA), Institut d'Imagerie Biomédicale (I²BM), NeuroSpin, CEA Saclay, Bât. 145, F-91191 Gif-sur-Yvette cedex, France

ARTICLE INFO

Article history:

Received 19 February 2010

Revised 11 May 2010

Available online 16 May 2010

Keywords:

Diffusion
Diffusion-weighting
Frequency-swept
Adiabatic
Pulses

ABSTRACT

In the present work, the non-linear phase dispersion induced by slice selective frequency-swept pulses is analyzed, in order to assess NMR signal attenuation due to molecular diffusion during such pulses. In particular, theoretical considerations show that diffusion-weighting can be calculated based on the non-linear phase spatial derivative (i.e. the phase gradient), and that the phase of B_1 field at the instant of the flip does not contribute to phase scrambling and diffusion-weighting, yielding a simple analytical expressions. The theory is validated by confrontation with numerical simulations of the Bloch equations including diffusion, performed for a pair of hyperbolic secant pulses and a pair of CHIRP pulses. The simple though general conceptual framework developed here should be useful for the understanding and the exact calculation of diffusion-weighting in NMR sequences using frequency-swept pulses.

© 2010 Elsevier Inc. All rights reserved.

1. Introduction

Adiabatic pulses provide an efficient way to perform broadband and homogeneous magnetization flip, even in the presence of strong B_1 inhomogeneities [1]. This property has for example been exploited to perform slice or volume selection, such as in the LASER spectroscopy sequence [2], in the Pseudo-LASER spectroscopic imaging sequence [3] or in various imaging sequences [4–7]. Furthermore, trains of adiabatic pulses may be used to generate contrasts based on relaxation in the rotating frame [8,9].

When applied in conjunction with a slice selection gradient, an adiabatic pulse generates a non-linear phase throughout the selected slice along the direction of the gradient. This is due to the frequency-swept nature of adiabatic pulses, where the magnetization is flipped when the frequency of the pulse is equal to the Larmor frequency Ω . This phase can then be refocused by a second, identical pulse [10,11], in order to prevent signal loss due to incoherent averaging throughout the slice. It has been argued that the phase dispersion created by an adiabatic pulse might induce diffusion-weighting. In their pioneer work [12], Sun and Bartha proposed an expression for diffusion-weighting induced by trains of hyperbolic secant pulses, assuming a quadratic phase dispersion (such as induced by a CHIRP pulse [13]).

When “zooming” into the elementary events occurring during frequency-swept pulses, two components can be identified in the

non-linear phase: the phase acquired in the slice selection gradient, depending on the gradient strength and on the instant of the flip t_Ω , and the phase induced by the B_1 field orientation itself, depending on the B_1 phase at the instant of the flip. In the present work, we propose to revisit the origins of the non-linear phase dispersion to assess if both the phase variation of the B_1 field during the sweep and the phase acquired in the slice selection gradient should be explicitly considered when calculating diffusion-weighting. To address these questions, a formalism is proposed that allows general calculation of diffusion-weighting when frequency-swept pulses are used. An analytical expression is then derived for diffusion-weighting induced by a pair of slice selective hyperbolic secant pulses and CHIRP pulses. These expressions are validated by numerical simulation of the Bloch equations including diffusion.

2. Theory

2.1. The phase induced during a frequency-swept pulse

An exact evaluation of the rotation induced by an arbitrary pulse requires composing rotation operators over suitably small time intervals to account for elementary rotations around a step-wise constant effective field, rapidly leading to complex analytical expressions. However, during a frequency-swept pulse, the magnetization can be assumed to be flipped around the B_1 field at the instant t_Ω when the frequency of the pulse is equal to its Larmor frequency Ω [3,6,7,14]. This approximation provides a simple yet accurate description of magnetization's behavior during the pulse,

* Corresponding author. Address: CEA Fontenay-aux-Roses, Bât. 61, 18 route du Panorama, F-92265 Fontenay-aux-Roses cedex, France.

E-mail address: julien.valette@cea.fr (J. Valette).

which was verified by many numerical simulations and experiments [3,6,7,14]. It allows for example the calculation of the magnetization's phase during the pulse [3,6,7,14]. Let us consider for example a frequency-swept pulse of duration T_p performing slice-selective refocusing. Considering a gradient of magnitude G_{slice} oriented along x , the phase evolution for magnetization with Larmor frequency $\Omega = \gamma G_{\text{slice}} x$ and flipped at t_{Ω} is given by [3,7], Φ_{B1} being the phase of the \mathbf{B}_1 field (Fig. 1):

$$\begin{aligned} 0 < t < t_{\Omega} : \phi(x, t) &= \gamma G_{\text{slice}} t x \\ t_{\Omega} < t < T_p : \phi(x, t) &= 2\phi_{B1}(t_{\Omega}) + \gamma G_{\text{slice}}(t - 2t_{\Omega})x \end{aligned} \quad (1)$$

This phase dispersion can then be refocused by a second, identical slice selective pulse. Looking at Eq. (1), two components can be identified in the non-linear phase: the phase acquired in the slice selection gradient, depending on the gradient strength and on the instant of the flip t_{Ω} , and the phase induced by the \mathbf{B}_1 field orientation itself, depending on the \mathbf{B}_1 phase at the instant of the flip. Since diffusion-weighting is based on phase scrambling, both components may *a priori* contribute to signal attenuation. Without further analysis, the effect of the \mathbf{B}_1 phase cannot be taken into account. We will now try to clarify how this \mathbf{B}_1 phase contributes to diffusion-weighting induced by frequency-swept pulses.

2.2. Diffusion in an arbitrary phase gradient

The usual definition of $\mathbf{k}(t)$ as the moment of a \mathbf{B}_0 gradient \mathbf{G} will be used:

$$\mathbf{k}(t) = \gamma \int_0^t \mathbf{G}(t') dt' \quad (2)$$

Using this notation, the signal attenuation due to diffusion during duration t in \mathbf{B}_0 gradients is (\mathbf{D} being the diffusion tensor):

$$A(t) = \exp\left(-\int_0^t \mathbf{k}^T(u) \times \mathbf{D} \times \mathbf{k}(u) du\right) \quad (3)$$

It is important to note that the phase induced by a gradient along x is $\phi(x, t) = k_x(t)x$, $k_x(t)$ being therefore the phase gradient $\partial\phi/\partial x$ (independent of x). Starting from here, let us consider now a more general case, where the phase $\phi(x, t)$ is not solely induced by \mathbf{B}_0 gradients, but by any other phenomenon, such as frequency-swept pulses. $\phi(x, t)$ is now an arbitrary function of x and t , with $\partial\phi/\partial x$ *a priori* depending on x and t . However, there is still a strong physical analogy between this arbitrary phase gradient $\partial\phi/\partial x$ and a \mathbf{B}_0 gradient moment k_x along x . Indeed, the effect of diffusion will be to scramble phase and induce signal loss, as induced by a \mathbf{B}_0 gradient. Using the gradient operator $\vec{\nabla}$, the phase gradient is given by:

$$\vec{\nabla}\phi(\mathbf{r}, t) = \left(\frac{\partial\phi}{\partial x}(\mathbf{r}, t), \frac{\partial\phi}{\partial y}(\mathbf{r}, t), \frac{\partial\phi}{\partial z}(\mathbf{r}, t)\right)^T \quad (4)$$

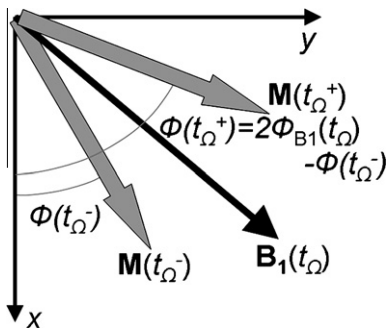


Fig. 1. Evolution of the transverse magnetization \mathbf{M} at the instant of the flip t_{Ω} during a 180° frequency-swept pulse. \mathbf{M} is considered to be instantaneously flipped by 180° around \mathbf{B}_1 .

It is demonstrated in Appendix A that, since ϕ can generally be considered locally linear (i.e. the phase gradient $\partial\phi/\partial x$ is constant) over the distance experienced by diffusing spins during the sequence (see Appendix B for the validity of this assumption), the attenuation due to diffusion is given by:

$$A(\mathbf{r}, t) = \exp\left(-\int_0^t \vec{\nabla}\phi^T(\mathbf{r}, u) \times \mathbf{D} \times \vec{\nabla}\phi(\mathbf{r}, u) du\right) \quad (5)$$

Therefore, there is a formal analogy between \mathbf{k} and $\vec{\nabla}\phi$ regarding diffusion-weighting. However, due to its more general form compared to Eq. (3), Eq. (5) can now be used to rigorously evaluate the effect of the phase induced by a frequency-swept pulse on diffusion-weighting.

2.3. Phase gradient induced during a frequency-swept pulse

The phase gradient evolution during the pulse is given by differentiating Eq. (1):

$$\begin{aligned} 0 < t < t_{\Omega} : \frac{\partial\phi}{\partial x} &= \gamma G_{\text{slice}} t = k_{\text{slice}}(t) \\ t_{\Omega} < t < T_p : \frac{\partial\phi}{\partial x} &= \underbrace{2 \frac{\partial\phi_{B1}}{\partial t}(t_{\Omega}) \frac{\partial t_{\Omega}}{\partial x}}_{k_{B1}} - 2\gamma G_{\text{slice}} x \frac{\partial t_{\Omega}}{\partial x} + \underbrace{\gamma G_{\text{slice}}(t - 2t_{\Omega})}_{k_{\text{slice}}(t)} \end{aligned} \quad (6)$$

In Eq. (6) two components can be identified: the usual slice gradient moment k_{slice} (whose sign is changed at t_{Ω} by the 180° rotation), and a “radiofrequency” term k_{B1} including \mathbf{B}_1 contribution. However, during frequency-swept pulses, the magnetization is flipped when the pulse frequency is equal to Ω , which can be written as $\partial\phi_{B1}/\partial t(t_{\Omega}) = \gamma G_{\text{slice}} x$. Inserting in Eq. (6) yields the following simplification:

$$\begin{aligned} 0 < t < t_{\Omega} : \frac{\partial\phi}{\partial x} &= \gamma G_{\text{slice}} t = k_{\text{slice}}(t) \\ t_{\Omega} < t < T_p : \frac{\partial\phi}{\partial x} &= \gamma G_{\text{slice}}(t - 2t_{\Omega}) = k_{\text{slice}}(t) \end{aligned} \quad (7)$$

In the end, the contribution of the \mathbf{B}_1 field orientation is cancelled out when calculating the spatial derivative of the non-linear phase, so that only the phase induced by the gradient needs to be considered for diffusion-weighting. In short, when considering diffusion-weighting, the effect of a 180° frequency-swept pulse is simply to change the sign of gradient moment \mathbf{k} at the instant t_{Ω} .

Note that a similar conclusion is reached if the pulse induces a 90° excitation rather than a 180° refocusing. Indeed, the phase is simply zero before the excitation ($0 < t < t_{\Omega}$), then the magnetization is instantaneously flipped around \mathbf{B}_1 and starts precessing for $t > t_{\Omega}$ [6]:

$$\begin{aligned} 0 < t < t_{\Omega} : \phi(x, t) &= 0 \\ t_{\Omega} < t < T_p : \phi(x, t) &= \phi_{B1}(t_{\Omega}) + \frac{\pi}{2} + \gamma G_{\text{slice}}(t - t_{\Omega})x \end{aligned} \quad (8)$$

In that case the phase gradient simplifies as well to:

$$\begin{aligned} 0 < t < t_{\Omega} : \frac{\partial\phi}{\partial x} &= 0 \\ t_{\Omega} < t < T_p : \frac{\partial\phi}{\partial x} &= \gamma G_{\text{slice}}(t - t_{\Omega}) = k_{\text{slice}}(t) \end{aligned} \quad (9)$$

3. Methods

3.1. Analytical calculation of diffusion-weighting during a pair of slice-selective frequency-swept pulses

Following the analysis detailed in the Theory section, diffusion-weighting induced during a pair of slice selective frequency-swept

pulses as shown on Fig. 2 (excluding potential spoiler gradients for simplicity) is easily calculated. It is simply the integral of $k_{slice}(t)^2$, which depends on t_{Ω} . Introducing the normalized instant of the flip $\alpha = 2t_{\Omega}/T_p - 1$ ($-1 < \alpha < 1$), and the delay Δ between the two pulses, integration of $k_{slice}(t)^2$ yields:

$$b = \gamma^2 G_{slice}^2 T_p^2 \left(\frac{T_p}{6} + \alpha^2 \left(\Delta - \frac{T_p}{2} \right) \right) \quad (10)$$

The above equation allows the evaluation of the diffusion-weighting factor b as a function of the position for arbitrary frequency-swept pulses when $\alpha(x)$ is known. For example, in the case of the CHIRP pulse, where the frequency-sweep is linear (THK being the slice thickness, x varying between $-THK/2$ and $THK/2$):

$$\alpha(x) = \frac{2x}{THK} \quad (11)$$

In the case of the hyperbolic secant pulse (HS1) [6], β being the cutoff factor of the pulse:

$$\alpha(x) = \frac{1}{2\beta} \log \left(\frac{1 + 2x/THK}{1 - 2x/THK} \right) \quad (12)$$

3.2. Numerical simulations

One-dimension numerical simulations of the Bloch equations were performed for the sequence of Fig. 2, using home-made programs written in Matlab (The Mathworks, Natick, MA, USA) on a 1.80 GHz personal laptop. Simulations were performed for a pair of slice-selective refocusing hyperbolic secant (HS1) pulses, and for a pair of slice-selective refocusing CHIRP pulses. Pulse parameters were pulse duration to bandwidth product $R = 60$ and pulse

duration $T_p = 1$ ms (and cutoff factor $\beta = 5.3$ for the HS1 pulse). The sequence parameters were echo time $TE = 10$ ms (i.e. $\Delta = 5$ ms), and slice thickness $THK = 1.5$ mm. Spins were assumed to be aligned along x at the beginning of the simulation. Time-step τ for the simulation was $1 \mu s$. Simulation was performed for one million diffusing spins, with diffusion coefficient $D = 5 \mu m^2/ms$. This was achieved by randomly displacing spins, at each time step during the course of Bloch simulation, over a distance equal to the square root of $2D\tau$, with a + or – sign randomly drawn for each spin's displacement. Total computing time for the 10^6 spins was ~ 130 h. The NMR signal was then evaluated over 500 pixels spanning the slice thickness, by averaging the transverse magnetization of spins present in each pixel at the end of the sequence. The reference signal to determine attenuation was simulated by setting $D = 0$, which allowed getting rid of imperfections in the slice selection profile (which was necessary for the CHIRP pulse which yielded non-flat profile). Simulation was compared to the theoretical diffusion-weighted signal obtained when inserting Eq. (11) (for the CHIRP pulse) and Eq. (12) (for the HS1 pulse) in Eq. (10), with signal attenuation equal to $\exp(-bD)$. This comparison was done over 90% only of slice thickness in order to exclude the transition bands. Note that the unusually high value for the diffusion coefficient ($D = 5 \mu m^2/ms$) was chosen to exacerbate signal attenuation, in order to facilitate comparison between theory and simulation.

4. Results and discussion

The simulated signal attenuation along the direction of the slice selective gradient is shown in Fig. 3A for the pair of HS1 pulses, and Fig. 3B for the pair of CHIRP pulses (over 90% of slice thickness to exclude the transition bands). Although the slice selection gradient

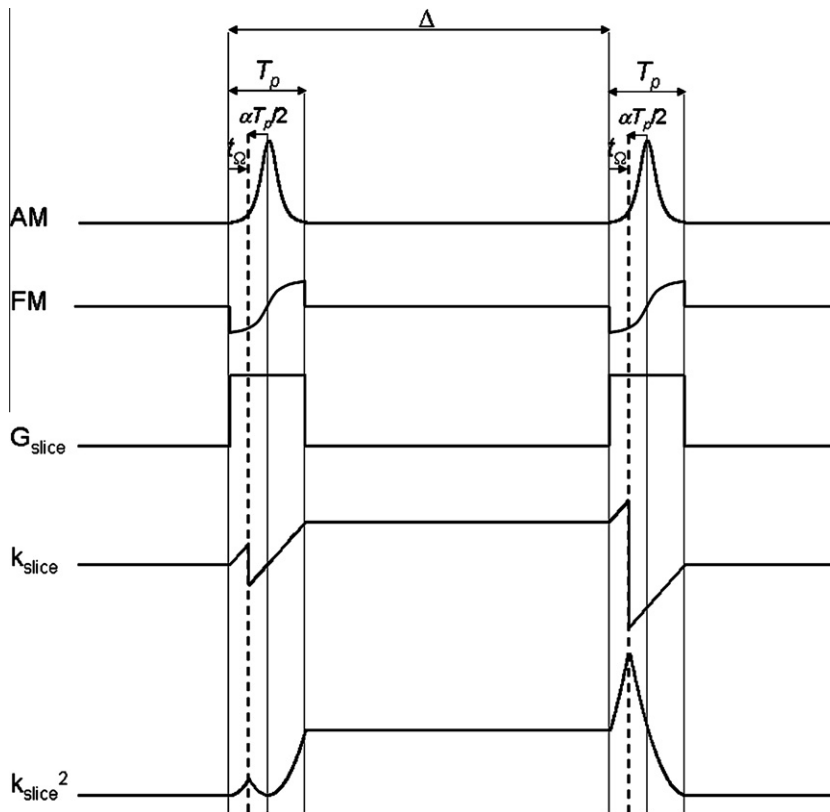


Fig. 2. Slice selective double spin echo sequence performed by frequency-swept pulses. Amplitude modulation (AM) and frequency modulation (FM) of the pulses are shown. Slice selection gradient G_{slice} is turned on only during the pulses. From the sequence chronogram, the time-evolution of k_{slice} and k_{slice}^2 can be easily calculated for a given instant of flip t_{Ω} , displayed here as a dashed vertical line. On the chronogram the normalized instant of flip $\alpha = 2t_{\Omega}/T_p - 1$ is also represented.

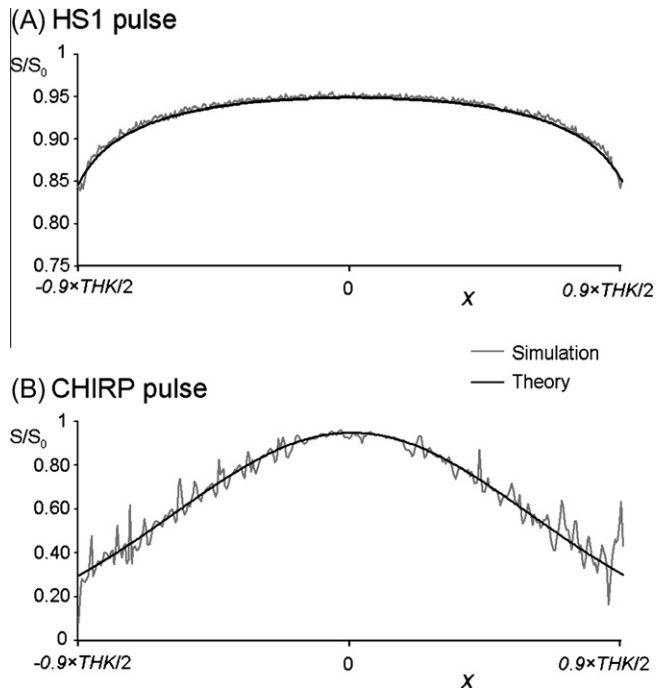


Fig. 3. Comparison between simulated (light gray line) and theoretical (black line) signal loss at the end of a pair of slice selective frequency-swept pulses shown in Fig. 2, for (A) hyperbolic secant HS1 pulses; and (B) CHIRP pulses. Signal attenuation profiles S/S_0 are plotted as a function of the position x along the thickness THK of the slice, over 90% of the bandwidth to exclude transition bands. For both situations, $R = 60$, $T_p = 1$ ms, $\Delta = 5$ ms, $THK = 1.5$ mm, $D = 5 \mu\text{m}^2/\text{ms}$.

is the same for both types of pulses, signal attenuation is much stronger for the CHIRP pulse, as soon as positions away from the center of the slice are considered. This is due to the fact that, for the HS1 pulse, the largest fraction of the slice's magnetization is flipped very close to the center of the pulse, which yields the smallest integral for $k_{\text{slice}}(t)^2$: 90% of the bandwidth is indeed swept during only $\sim 30\%$ of the pulse duration (i.e. $|\alpha| < 0.3$ for 90% of the slice thickness).

In both cases, simulations agrees very well with the theoretical predictions, demonstrating: (i) the validity of the theory based on phase gradients (Eq. (5)); (ii) the fact that the phase dispersion induced by the phase variation of the \mathbf{B}_1 field during the frequency sweep vanishes when considering the effect of this phase on diffusion-weighting (Eq. (7)); and (iii) the analytical expression of diffusion-weighting induced by a pair of frequency-swept pulses (Eq. (10)).

In our opinion, beyond its conceptual simplicity, the main interest of using phase gradients as a basis for b -values calculations is that it allows taking into account diffusion during the pulse. In addition, exact calculation of cross-terms between the phase gradient induced by the slice selective frequency-swept pulse and other phase gradients (such induced by as \mathbf{B}_0 inhomogeneity or spoiler gradients) is made possible by integration during the pulse. By contrast, in their original paper [12], Sun and Bartha considered only the phase induced at the end of the pulse, which was therefore considered to be executed instantaneously, precluding exact calculation of diffusion effects during the pulse.

An important point of our analysis is that, when considering diffusion-weighting, the effect of a 180° frequency-swept pulse is simply to change the sign of the gradient moment \mathbf{k} at the instant t_Ω , without any intrinsic effect of the \mathbf{B}_1 phase modulation on the signal attenuation. In other words, a slice selective frequency-swept pulse will never induce a stronger diffusion-weighting than

the sole slice selection gradient. This maximal diffusion-weighting is only achieved for spins at the very edges of the slice, which are flipped at the very beginning or the very end of the flip (which is for example visible in Eq. (10), where $\alpha = \pm 1$ leads to the usual attenuation factor $\gamma^2 G^2 \delta^2 (\Delta - \delta/3)$ for bipolar gradient pulses of duration $\delta = T_p$ separated by Δ). The phase gradient appears to be a fundamental parameter when considering diffusion-weighting induced by frequency-swept pulses. Interestingly, this echoes a previous work where we already reported the relevance of phase gradient to characterize the accuracy of Fourier transformed MRI and spectroscopic imaging when performing volume selection by unpaired adiabatic pulses [3]. In that work, phase gradient was also used to generate a “sliding apodization window” to perform spatial apodization on a pixel-per-pixel basis. Note that, in order to calculate phase gradient, we used to explicitly calculate $\Phi(x)$ (i.e. including the \mathbf{B}_1 phase, see Eq. (1)), before differentiating it. In the present work, Eq. (7) (and subsequent Eq. (B3), cf. Appendix B) provides a new, simplified way to calculate the phase gradient, where the \mathbf{B}_1 phase is not involved anymore.

Although very general, the formalism proposed here is valid provided the phase induced by the pulse can be considered “locally” linear, “locally” meaning here within the distance traveled by spins during the diffusion time. As shown in Appendix B, this is in general valid, even for thin slices and pulses with high R factors. However, for some extreme situations (such as microscopic imaging), this assumption may not be correct anymore, resulting in phase scrambling between regions outside the linearity area.

5. Conclusion

In this work, diffusion-weighting induced by slice-selective frequency-swept pulses was described using the spatial gradient of the non-linear phase induced by the pulses. It was shown that phase gradients can be substituted for the magnetic field gradient moment \mathbf{k} in the equation describing signal attenuation due to diffusion (Eqs. (3) and (5)), yielding a convenient way to calculate diffusion-weighting induced by frequency-swept pulses. It was then shown that the phase gradient does not explicitly depend on the phase of the \mathbf{B}_1 field: in the end, as far as diffusion-weighting is concerned, the effect of a refocusing frequency-swept pulse is simply to change the sign of \mathbf{k} at the time of the flip. This simple result allows an exact calculation of diffusion-weighting induced by frequency-swept pulses, and should be useful for NMR sequences involving such pulses.

Appendix A. Signal attenuation in a phase gradient

The time evolution of the complex transverse magnetization Ψ including diffusion in an arbitrary phase field $\phi(\mathbf{r}, t)$ can be derived from the Bloch-Torrey equation, writing the frequency under its general form $\partial\Phi/\partial t$ (ignoring relaxation):

$$\frac{\partial \Psi}{\partial t} = i \frac{\partial \phi}{\partial t} \Psi + \vec{\nabla} \cdot (\mathbf{D} \times \vec{\nabla} \Psi) \quad (\text{A1})$$

A solution to this differential equation can be searched, in a small volume dV around position \mathbf{r} , under the form:

$$\Psi(\mathbf{r}, t) = m_0 A(t) \exp(i\phi(\mathbf{r}, t)) \quad (\text{A2})$$

In Eq. (A2), m_0 is the magnetization density, which is assumed to be constant in dV . $A(t)$ is the attenuation factor originating from diffusion. It does not explicitly depend on the position since it is assumed here that the phase derivative can be considered constant in dV , which means that the effect of phase scrambling is homogeneous within the volume considered, as it is assumed when phase

is induced by \mathbf{B}_0 gradient. A more detailed analysis about the validity of this assumption is performed in Appendix B. Injecting Eq. (A2) in Eq. (A1) yields:

$$\frac{\partial A(t)}{\partial t} \exp(i\phi(\mathbf{r}, t)) = iA(t) \vec{\nabla} \cdot (\mathbf{D} \times \vec{\nabla}(\exp(i\phi(\mathbf{r}, t)))) \quad (\text{A3})$$

Assuming again that the phase is locally linear within dV (i.e. all second order phase derivatives are zero), the two successive gradient operators in Eq. (A3) simplify to:

$$\vec{\nabla} \cdot (\mathbf{D} \times \vec{\nabla}(\exp(i\phi(\mathbf{r}, t)))) = i \exp(i\phi(\mathbf{r}, t)) \vec{\nabla} \phi^T \times \mathbf{D} \times \vec{\nabla} \phi \quad (\text{A4})$$

Re-injecting this expression in Eq. (A4) finally yields:

$$\frac{\partial A(t)}{\partial t} = -A(t) \vec{\nabla} \phi^T \times \mathbf{D} \times \vec{\nabla} \phi \quad (\text{A5})$$

Solving Eq. (A5) ultimately yields the time evolution of the attenuation factor resulting from diffusion in an arbitrary time varying phase gradient in a small volume dV around \mathbf{r} (with $A(0) = 1$):

$$A(t) = \exp\left(-\int_0^t \vec{\nabla} \phi^T(u) \times \mathbf{D} \times \vec{\nabla} \phi(u) du\right) \quad (\text{A6})$$

Appendix B. Local linearity of the phase induced by frequency-swept pulses

The phase at a distance λ from position x_0 can be expressed as a Taylor expansion:

$$\phi(x_0 + \lambda) = \phi(x_0) + \frac{\partial \phi}{\partial x}(x_0)\lambda + \frac{1}{2} \frac{\partial^2 \phi}{\partial x^2}(x_0)\lambda^2 + \dots \quad (\text{B1})$$

As far as diffusion-weighting is concerned, assuming local linearity is equivalent to say that the second- and higher-order derivative terms are negligible over the length scale of the diffusion. Indeed, under this condition, no significant phase scrambling and subsequent signal loss can occur due to these terms. In that context, the distance λ to consider is the average distance traveled by spins during the diffusion time T_d during which the phase is not refocused (i.e. $\lambda^2 = 2DT_d$, D being the diffusion coefficient). For the second-order derivative, this condition can be expressed as:

$$DT_d \left| \frac{\partial^2 \phi}{\partial x^2} \right| \ll \pi \quad (\text{B2})$$

Taking the expression for $\partial\phi/\partial x$ as given in Eq. (7), introducing the normalized instant of flip $\alpha = 2t_\Omega/T_p - 1$ ($-1 < \alpha < 1$), and considering the phase derivative at the end of the pulse:

$$\frac{\partial \phi}{\partial x} = \gamma G_{\text{slice}}(T_p - 2t_\Omega) = -\gamma G_{\text{slice}} T_p \alpha(x) \quad (\text{B3})$$

Differentiating Eq. (B3), introducing the pulse duration to bandwidth product R , and the slice thickness THK , and injecting in Eq. (B2) ultimately results in the following condition:

$$R \frac{2DT_d}{THK} \left| \frac{\partial \alpha}{\partial x} \right| \ll 1 \quad (\text{B4})$$

For a CHIRP pulse, $\alpha(x) = 2x/THK$, which yields the following condition:

$$R \frac{4DT_d}{THK^2} \ll 1 \quad (\text{B5})$$

For a HS1 pulse, $\alpha(x)$ is given by Eq. (11) [6]. Differentiation of α and injection in Eq. (B4) leads to:

$$R \frac{4DT_d}{THK^2} \left| \frac{1}{1 - 4x^2/THK^2} \right| \frac{1}{\beta} \ll 1 \quad (\text{B6})$$

Limiting the analysis to 90% of the slice thickness to exclude transition bands yields the following condition (for the extreme value reached at $x = \pm 0.9 \times THK/2$):

$$\frac{5.3}{\beta} R \frac{4DT_d}{THK^2} \ll 1 \quad (\text{B7})$$

Taking the usual value for the truncation factor $\beta = 5.3$ finally results in a condition which is similar for CHIRP and HS1 pulses. In general, this condition will always be satisfied. For example, taking $D = 2.5 \mu\text{m}^2/\text{ms}$, $T_d = 20$ ms, $R = 60$ and $THK = 1$ mm, results in the left-hand side of Eqs. (B5)–(B7) being equal to ~ 0.01 . This illustrates that, in the vast majority of situations, the phase induced by frequency-swept pulses can be considered linear, as far as diffusion-weighting is considered.

References

- [1] M.S. Silver, R.I. Joseph, D.I. Hoult, Highly selective $\pi/2$ and π pulse generation, *J. Magn. Reson.* 59 (1984) 347–351.
- [2] M. Garwood, L. Delabarre, The return of the frequency sweep: designing adiabatic pulses for contemporary NMR, *J. Magn. Reson.* 153 (2001) 155–177.
- [3] J. Valette, J.Y. Park, O. Grohn, K. Ugurbil, M. Garwood, P.G. Henry, Spectroscopic imaging with volume selection by unpaired adiabatic pi pulses: theory and application, *J. Magn. Reson.* 189 (2007) 1–12.
- [4] R. Gruetter, I. Tkac, Field mapping without reference scan using asymmetric echo-planar techniques, *Magn. Reson. Med.* 43 (2000) 319–323.
- [5] C.R. Jack Jr., M. Garwood, T.M. Wengenack, B. Borowski, G.L. Curran, J. Lin, G. Adriany, O.H. Grohn, R. Grimm, J.F. Poduslo, In vivo visualization of Alzheimer's amyloid plaques by magnetic resonance imaging in transgenic mice without a contrast agent, *Magn. Reson. Med.* 52 (2004) 1263–1271.
- [6] J.Y. Park, L. Delabarre, M. Garwood, Improved gradient-echo 3D magnetic resonance imaging using pseudo-echoes created by frequency-swept pulses, *Magn. Reson. Med.* 55 (2006) 848–857.
- [7] J.Y. Park, M. Garwood, Spin-echo MRI using $\pi/2$ and π hyperbolic secant pulses, *Magn. Reson. Med.* 61 (2009) 175–187.
- [8] S. Michaeli, D.J. Sorce, D. Idiyatullin, K. Ugurbil, M. Garwood, Transverse relaxation in the rotating frame induced by chemical exchange, *J. Magn. Reson.* 169 (2004) 293–299.
- [9] H.I. Grohn, S. Michaeli, M. Garwood, R.A. Kauppinen, O.H. Grohn, Quantitative T(1rho) and adiabatic Carr-Purcell T2 magnetic resonance imaging of human occipital lobe at 4 T, *Magn. Reson. Med.* 54 (2005) 14–19.
- [10] S. Conolly, G. Glover, D. Nishimura, A. Macovski, A reduced power selective adiabatic spin-echo pulse sequence, *Magn. Reson. Med.* 18 (1991) 28–38.
- [11] K. Stott, J. Stonehouse, J. Keeler, T.L. Hwang, A.J. Shaka, Excitation sculpting in high-resolution nuclear magnetic resonance spectroscopy: application to selective NOE experiments, *J. Am. Chem. Soc.* 117 (1995) 4199–4200.
- [12] Z. Sun, R. Bartha, Enhanced diffusion weighting generated by selective adiabatic pulse trains, *J. Magn. Reson.* 188 (2007) 35–40.
- [13] D. Kunz, Use of frequency-modulated radiofrequency pulses in MR imaging experiments, *Magn. Reson. Med.* 3 (1986) 377–384.
- [14] J.G. Pipe, Spatial encoding and reconstruction in MRI with quadratic phase profiles, *Magn. Reson. Med.* 33 (1995) 24–33.